WZ and W+jets production at large transverse momenta beyond NLO

SEBASTIAN SAPETA
Institute for Particle Physics Phenomenology, Durham University, South Rd, Durham DH1 3LE, UK

We present a study of higher order QCD corrections beyond NLO to processes with electroweak vector bosons. We focus on the regions of high transverse momenta of commonly used differential distributions. We employ the LoopSim method, combined with NLO packages, VBFNLO and MCFM, to merge the NLO samples with different multiplicities, in order to compute the dominant part of the NNLO corrections at high p_T. We find that these corrections are indeed substantial, in the 30%-100% range, for a number of experimentally relevant observables. For other observables, they lead to significant reduction of scale uncertainties.

1 Introduction

The production of electroweak vector bosons forms one of the most important class of Standard Model (SM) processes. W boson in association with jets is a background to single and pair top production, diboson production, Higgs production as well as to searches for physics beyond the standard model (BSM). The same is true for the processes with two electroweak bosons in the final state, like WZ production, which, in addition, are sensitive to anomalous triple gauge boson coupling (TGC). The above processes are also interesting in their own right as they provide important tests of quantum chromodynamics (QCD).

In this proceedings, we present a study of WZ and W+jets processes, at the LHC energies, at approximate next-to-next-to-leading order (NNLO) in QCD. The motivation to go beyond the next-to-leading order (NLO) for those processes comes from the fact that the NLO corrections for WZ and W+jets turn out to be sizable for a number of important distributions at high transverse momentum. This corrections come about due to new production channels and new topologies absent at leading order (LO) and appearing only at NLO. An example, for the case of WZ, is shown in Fig. 1. At leading order, the production of dibosons is possible only via $q\bar{q}$ channel. At NLO, the new qg channel, with enhanced partonic luminosity, opens up and dominates the LO contribution. Similarly, at LO, only back-to-back WZ configurations are possible whereas at NLO, an electroweak boson can recoil against a parton and the other boson can be soft or collinear, which brings logarithmic enhancements for a number of distributions.

Because the NLO corrections often turn out to dominate the leading order, it is of great importance to try to assess the NNLO corrections, to check the convergence of the perturbative series, and to obtain precise and stable results. As shown in the right diagram of Fig. 1, in the case of WZ production, one can also expect genuinely new sub-processes and topologies appearing for the first time at NNLO.

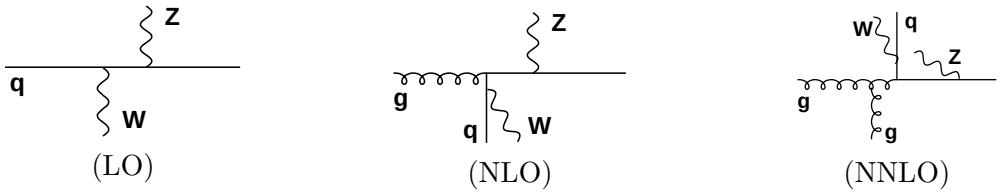

Figure 1: Example diagrams contributing to WZ production at LO, NLO and NNLO.

2 Details of the calculations

To compute the dominant part of the NNLO QCD corrections to WZ and W+jets processes, we used the LoopSim method [1] together with the NLO packages VBFNLO [2] and MCFM. [3]

LoopSim allows for a consistent merging of WZ and WZj NLO samples to obtain the result for WZ at $\bar{n}$NLO, where $\bar{n}$ denotes the approximate 2-loop contribution determined from the real and 1-loop parts of WZj at NLO. Similarly, Wj and Wjj NLO samples are used to compute the results for W+jets at $\bar{n}$NLO. The method is based on unitarity and it is supposed to work best for processes and observables with large NLO K-factors from new topologies, as $\sigma_{\bar{n}\mathrm{NLO}} - \sigma_{\mathrm{NNLO}} \sim \frac{1}{K}$. LoopSim has one parameter, R_{LS}, which affects the way the procedure assigns branching structure to the original NLO sample. By default, we set $R_{\mathrm{LS}} = 1$ and vary it by ± 0.5, to probe the related uncertainties. As we shall see, they are much smaller then the factorization and renormalization scale uncertainties at high p_T.

3 Results

The WZ production process was studied [4] with the following cuts: The charged leptons were required to be hard and central: $p_{T,\ell} \geq 15(20)$, for ℓ coming from Z(W), and $|y_\ell| \leq 2.5$. The missing transverse energy had to satisfy the cut $E_{T,\mathrm{miss}} > 30\,\mathrm{GeV}$. The same-flavor lepton pair mass had to lie in the window $60 < m_{l^+l^-} < 120\,\mathrm{GeV}$. The final state partons with $|y_p| \leq 5$ were clustered to jets with the anti-k_t algorithm with the radius $R = 0.45$. For the central value of the factorization and renormalization scales, we chose $\mu_{F,R} = \frac{1}{2}\sum p_{T,\mathrm{partons}} + \frac{1}{2}\sqrt{p_{T,W}^2 + m_W^2} + \frac{1}{2}\sqrt{p_{T,Z}^2 + m_Z^2}$. All WZ results correspond to the sum of contributions from two unlike flavor decay channels, $ee\mu\nu_\mu$ and $\mu\mu e\nu_e$, and both $\mathrm{W^+Z}$ and $\mathrm{W^-Z}$ production channels.

Fig. 2 (left) shows the differential distribution, at $\sqrt{s} = 8\,\mathrm{TeV}$, of the effective mass observable defined as

$$H_T = \sum p_{T,\mathrm{jets}} + \sum p_{T,l} + E_{T,\mathrm{miss}}\,. \tag{1}$$

As a first check, we computed the H_T distribution at $\bar{n}$LO, which can be directly compared with the exact NLO result. As we see in Fig. 2, $\bar{n}$LO matches very well the NLO at high H_T, providing the correct prediction for the large K factor, of the order of 10. The H_T observable is therefore very well suited to be studied with LoopSim. The $\bar{n}$NLO result shown in Fig. 2 yields up to 100% correction with respect to NLO. We see that the R_{LS} uncertainty is negligible at high H_T and the scale uncertainty decreases only a little at $\bar{n}$NLO. The latter is related to the fact that this observable favours new topologies that enter only at NNLO and are computed with LO accuracy (cf. the right diagram of Fig. 1).

In Fig. 2 (right), we present the distribution of the lepton with maximum p_T at $\sqrt{s} = 14\,\mathrm{TeV}$. Also here, the $\bar{n}$NLO corrections are large and beyond the NLO scale uncertainty already at 200 GeV. In addition, for this observable, we show the results with veto on the jets with $p_T > 50\,\mathrm{GeV}$. We observe that the $\bar{n}$NLO corrections with veto are negative, go beyond the NLO scale uncertainty, and exhibit larger uncertainties due to renormalization and factorization scale

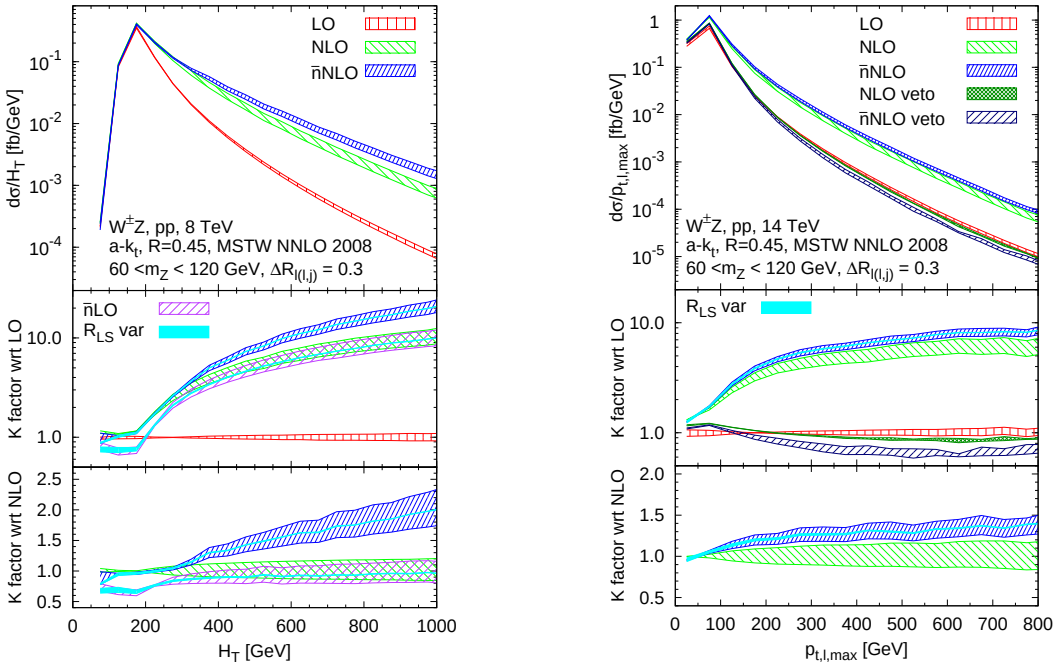

Figure 2: WZ production at the LHC. Differential cross sections and K factors for H_T, defined in Eq. (1), at $\sqrt{s} = 8\,\text{TeV}$ (left) and for the p_T of the hardest lepton at $\sqrt{s} = 14\,\text{TeV}$ (right). The bands correspond to varying $\mu_F = \mu_R$ by factors 1/2 and 2 around the central value. The cyan solid bands give the uncertainty related to R_{LS} varied between 0.5 and 1.5. The distribution is a sum of contributions from two unlike flavor decay channels.

variation than the NLO result. The latter indicates that the small scale uncertainty at NLO was partially accidental. Overall, these results clearly illustrate that the veto procedure should be used with great care as it has a non-trivial effect on the convergence of the perturbative series.

The W+jets process was studied with the cuts that match the ATLAS measurement. [5] The charged leptons were required to have $p_{T,\ell} \geq 20\,\text{GeV}$ and $|y_\ell| \leq 2.5$. The missing transverse energy had to be above $E_{T,\text{miss}} > 25\,\text{GeV}$. The transverse mass [5] of the W was required to be greater than 40 GeV. Only events with anti-k_t, R=0.4 jets with $p_{T,\,\text{jet}} > 30\,\text{GeV}$ and $|y_{\,\text{jet}}| < 4.4$ were accepted. Finally, for each jet, its distance to the lepton $\Delta R(\ell,\,\text{jet})$ had to be greater than 0.5, otherwise this jet was removed from the event. For the central value of the factorization and the renormalization scale, we chose $\mu_{F,R} = \frac{1}{2}\hat{H}_T = \frac{1}{2}\left(\sum p_{T,\text{partons}} + \sum p_{T,\text{leptons}}\right)$.

In Fig. 3 we show the differential distributions of the transverse momentum of the hardest jet (left) and the scalar sum of the traverse momenta of jets, leptons and missing energy, H_T (right), defined previously in Eq. (1). The results correspond $\sqrt{s} = 7\,\text{TeV}$ and are sums of contributions from W^+ and W^- for a single lepton decay channel $W \to \ell\nu$. The theoretical predictions, computed at LO, NLO and $\bar{n}$NLO, were corrected for non-perturbative effects. [5]

In the case of the p_T of the leading jet, we see a substantial reduction of scale uncertainty at $\bar{n}$NLO, while the result stays within the NLO band. Hence, that observable comes under control at $\bar{n}$NLO as no new channel or topologies appear at this order. We also note that the R_{LS} uncertainty is always smaller that the scale uncertainty and it decreases with increasing p_T. For the H_T distribution, the $\bar{n}$NLO result goes beyond the NLO uncertainty band for $H_T > 300\,\text{GeV}$ and the corrections are up to 30% with respect to NLO. The R_{LS} uncertainty is negligible above 300 GeV. The large $\bar{n}$NLO correction to H_T is a result of the third jet coming from the initial state radiation. This jet adds a small contribution to H_T but, because the spectrum is steeply falling, the enhancement in the distribution is substantial. Altogether, the $\bar{n}$NLO result, by including configurations with three partons in the final state, describes the H_T data significantly better than NLO.

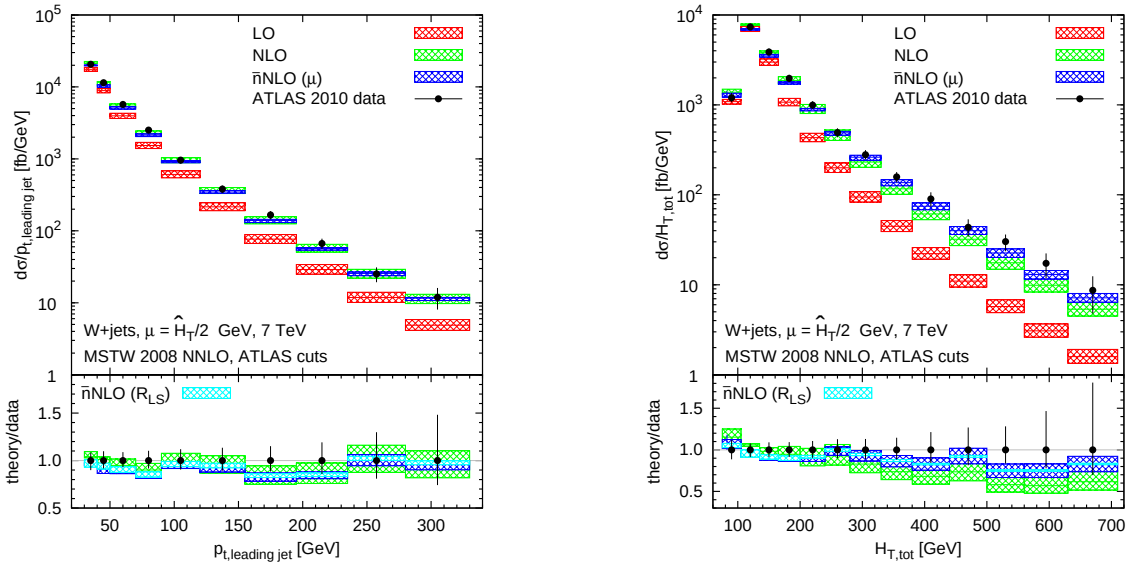

Figure 3: W+jets production at the LHC, $\sqrt{s} = 7\,\text{TeV}$. Differential cross sections as functions of the p_T of the hardest jet (left) and H_T (right) at LO, NLO and $\bar{n}$NLO. The theoretical results are corrected for non-perturbative effects and are compared to the ATLAS data. The bands correspond to varying $\mu_F = \mu_R$ by factors 1/2 and 2 around the central value. The cyan solid bands give the uncertainty related to R_{LS} varied between 0.5 and 1.5.

4 Conclusions

We used LoopSim together with VBFNLO and MCFM to compute approximate NNLO corrections to processes with vector bosons: WZ and W+jets production. Our results, referred to as $\bar{n}$NLO, are expected to account for the dominant part of the NNLO QCD corrections in some high p_T distributions.

In the case of WZ production, we found sizable effects due to $\bar{n}$NLO for a range of experimentally relevant observables: H_T, $p_{T,\ell,\text{max}}$, $E_{T,\,\text{miss}}$.[4] They all show non-trivial kinematic dependencies and go beyond NLO uncertainty bands. For W+jets, the H_T-type observables exhibit large $\bar{n}$NLO corrections. On the other hand, p_T of the leading jet, which gets large correction at NLO, nicely converges at $\bar{n}$NLO and shows significant reduction of scale uncertainty.

In conclusion, the QCD corrections beyond NLO to process with electroweak bosons are in many cases sizable and should be taken into account in precision studies as well as in searches for new physics.

Acknowledgments

We thank the organizers of the 48$^{\text{th}}$ Rencontres de Moriond for the opportunity to present these results and for financial support. The studies described here were performed in collaboration with Francisco Campanario, Daniel Maitre and Gavin Salam.

References

1. M. Rubin, G. P. Salam and S. Sapeta, JHEP **1009**, 084 (2010).
2. K. Arnold, J. Bellm, G. Bozzi, F. Campanario, C. Englert, B. Feigl, J. Frank and T. Figy *et al.*, *Comput. Phys. Commun.* **180**, 1661 (2009)
3. J. M. Campbell and R. K. Ellis, *Phys. Rev.* D **60**, 113006 (1999), `http://mcfm.fnal.gov`
4. F. Campanario and S. Sapeta, *Phys. Lett.* B **718**, 100 (2012)
5. G. Aad *et al.* [ATLAS Collaboration], *Phys. Rev.* D **85**, 092002 (2012).